

Accepted for publication in ApJ

## X-ray Selected Intermediate-Redshift Groups of Galaxies

John S. Mulchaey

*The Observatories of the Carnegie Institution of Washington, 813 Santa Barbara St., Pasadena, 91101*

[mulchaey@ociw.edu](mailto:mulchaey@ociw.edu)

Lori M. Lubin, Chris Fassnacht

*Department of Physics, University of California at Davis, 1 Shields Avenue, Davis, CA 95616*

Piero Rosati

*European Southern Observatory, Karl-Schwarzschild-Strasse 2, D-85748 Garching, Germany*

and

Tesla E. Jeltema

*The Observatories of the Carnegie Institution of Washington, 813 Santa Barbara St., Pasadena, 91101*

## ABSTRACT

We present spectroscopic confirmation of nine moderate redshift galaxy groups and poor clusters selected from the *ROSAT* Deep Cluster Survey. The groups span the redshift range  $z \sim 0.23 - 0.59$  and have between 4 and 20 confirmed members. The velocity dispersions of these groups range from  $\sim 125$  to  $650 \text{ km s}^{-1}$ . Similar to X-ray groups at low redshift, these systems contain a significant number of early-type galaxies. Therefore, the trend for X-ray luminous groups to have high early-type fractions is already in place by at least  $z \sim 0.5$ . In four of the nine groups, the X-ray emission is clearly peaked on the most luminous early-type galaxy in the group. However, in several cases the central galaxy is composed of multiple luminous nuclei, suggesting that the brightest group galaxy may still be undergoing major mergers. In at least three

(and possibly five) of the groups in our sample, a dominant early-type galaxy is not found at the center of the group potential. This suggests that many of our groups are not dynamically evolved despite their high X-ray luminosities. While similar systems have been identified at low redshift, the X-ray luminosities of the intermediate redshift examples are one to three orders of magnitude higher than those of their low redshift counterparts. We suggest that this may be evidence for group downsizing: while massive groups are still in the process of collapsing and virializing at intermediate redshifts, only low-mass groups are in the process of forming at the present day.

*Subject headings:* galaxies: clusters: general — galaxies: elliptical and lenticular, cD — galaxies: evolution

## 1. Introduction

Groups of galaxies constitute the most common galaxy associations, containing as many as 50–70% of all galaxies (Turner & Gott 1976; Geller & Huchra 1983; Eke et al. 2006). They are, therefore, an important laboratory for studying the processes associated with galaxy formation and evolution. In recent years, optical and X-ray studies of groups at low redshift have provided new insights into these important systems. In particular, there are strong correlations between the morphological composition of the luminous galaxies, the velocity dispersion, and the presence of X-ray emission (Zabludoff & Mulchaey 1998; Mulchaey & Zabludoff 1998; Mulchaey et al. 2003; Osmond & Ponman 2004). Specifically, diffuse X-ray emission is found almost exclusively in those groups dominated by early-type galaxies. In turn, the early-type fraction is strongly correlated with the group velocity dispersion and, thus, the group mass.

In the most luminous X-ray groups, the brightest group galaxy (BGG) is always a very massive elliptical, located at the peak of the X-ray emission (Ebeling, Voges & Böhringer 1994; Mulchaey et al. 1996; Mulchaey & Zabludoff 1998; Helson & Ponman 2000; Mulchaey et al. 2003; Osmond & Ponman 2004). As the peak of the X-ray emission is likely coincident with the center of the group, this implies that the BGG lies at the center of the group potential. Indeed, the position of the BGG is also indistinguishable from the center of the group potential as defined by the mean velocity and projected spatial distribution of the galaxies (Zabludoff & Mulchaey 1998). The fact that the BGG is located at the center of the potential suggests the formation of the BGG is intimately linked to the formation and evolution of the group itself.

Given their relatively low velocity dispersions, groups of galaxies provide ideal sites for galaxy-galaxy mergers (Barnes 1985; Aarseth & Fall 1980; Merritt 1985; Miles et al. 2004; Taylor & Babul 2005; Temporin & Fritze-von Alvensleben 2006). This implies that significant changes in the star formation rates and morphological appearance of galaxies may be occurring in groups. To better understand how galaxies evolve in the group environment, groups must be observed over a wide range of cosmic time. However, observations of groups at even moderate redshifts have been limited because of the difficulty of finding groups given their low galaxy densities. Allington-Smith et al. (1993) photometrically selected a sample of groups at intermediate redshifts by targeting known radio galaxies. Their study suggested a progressive bluing in the galaxy population. Small samples of groups at higher redshifts have also been found in deep redshift surveys (Lubin, Postman & Oke 1998; Cohen et al. 2000) and around lensed quasars (Rusin et al. 2001; Fassnacht & Lubin 2002; Nair 2002; Raychaudhury, Saha & Williams 2003; Grant et al. 2004; Faure et al. 2004; Williams et al. 2006). The recent completion of very large redshifts surveys now allow large group samples to be kinematically-defined from moderate redshifts up to  $z \sim 1$  (Carlberg et al. 2001; Gerke et al. 2005). Wilman et al. (2005a,b) studied a large sample of groups at moderate redshifts selected from the CNOC2 survey and found that the fraction of group members undergoing significant star formation increases strongly with redshift out to  $z \sim 0.5$ . Therefore, there is evidence for some evolution in the group environment in the last  $\sim 5$  billion years at least among optically-selected group samples.

X-ray emission from the hot intragroup medium provides another way to identify candidate groups at high redshifts. *ROSAT* was the first X-ray telescope capable of finding such systems and large numbers of group candidates at intermediate redshifts were found in deep surveys with this telescope (Rosati et al. 1995; Scharf et al. 1997; Burke et al. 1997; Rosati et al. 1998; Jones et al. 1998; Vikhlinin et al. 1998; Romer et al. 2000; Adami et al. 2000; Perlman et al. 2002; Jones et al. 2002; Burke et al. 2003). The *ROSAT* surveys suggest there is little or no evolution of the X-ray luminosity function of groups and poor clusters out to at least  $z=0.5$ . More recently, Willis et al. (2005) arrived at a similar conclusion using twelve groups and clusters from the early data taken as part of the *XMM* Large-Scale Structure (LSS) Survey. Upon completion, the *XMM*-LSS survey will provide a large sample of X-ray selected groups and poor clusters out to redshifts of  $z \sim 0.6$  or higher.

In this paper, we provide the first results from an extensive multi-wavelength study of nine X-ray selected galaxy groups and poor clusters in the redshift range  $0.2 < z < 0.6$  selected from deep *ROSAT PSPC* pointings. Our data allow the first detailed look at the morphological composition of X-ray groups at intermediate redshifts. A detailed study of the X-ray properties of six of these systems based on *XMM-Newton* observations is provided in a companion paper (Jeltema et al. 2006; hereafter Paper II). We assume a  $\Lambda$  cold dark

matter cosmology with  $\Omega_m=0.27$ ,  $\Lambda=0.73$ , and  $H_0=70 \text{ km s}^{-1} \text{ Mpc}^{-1}$  throughout this paper.

## 2. Sample Selection

We select our intermediate redshift group candidates from the *ROSAT* Deep Cluster Survey (RDCS; (Rosati et al. 1998)). As the deepest of the *ROSAT* pointing surveys, the RDCS is the best suited for selecting low luminosity systems (i.e. groups) at intermediate redshifts. The RDCS used a wavelet-based technique to search for extended sources in deep *ROSAT PSPC* pointings. A full description of the X-ray analysis and object selection technique is provided in Rosati et al. (1995). To identify the poorest galaxy systems in the RDCS, we restrict our sample to objects with X-ray luminosities between  $\sim 2 \times 10^{42} h_{70}^{-2} \text{ ergs s}^{-1}$  and  $\sim 2 \times 10^{43} h_{70}^{-2} \text{ ergs s}^{-1}$  in the 0.5–2 keV band. This corresponds to the range of nearby X-ray luminous groups (Mulchaey et al. 2003; Osmond & Ponman 2004). As we are interested in moderate redshift groups, we further restrict our sample to objects at  $z > 0.2$ . Figure 1 shows the distribution of redshifts and X-ray luminosities for RDCS groups as defined above. The majority of the systems are at the low redshift end ( $0.2 < z < 0.3$ ) as is expected from a flux-limited X-ray survey. However, for our initial study we have concentrated mostly on the  $z > 0.3$  groups, as these provide the longest time baseline for comparison with nearby groups. Furthermore, we have obtained *XMM-Newton* data primarily for the highest luminosity systems, as these targets tend to require the shortest exposure times.

Figure 2 shows contours of the diffuse X-ray emission overlaid on optical images of the six fields for which we have *XMM-Newton* data (Paper II). The three systems with only *ROSAT* data are shown in Figure 3. The association of the X-ray emission with an overdensity of galaxies is apparent in many cases.

## 3. Observations

### 3.1. Spectroscopic Data

To determine group membership, we obtained optical spectra for galaxies in each field using multi-object spectrographs at the Palomar, Las Campanas and Keck Observatories. Spectroscopic candidates for each group were selected from the original R or I band images taken for the RDCS with the KPNO and CTIO 4m telescopes. The program SExtractor (Bertin & Arnouts 1996) was used to classify objects as stars or galaxies and to measure magnitudes. For the present work, we considered all objects with a “stellarity-index” of

less than 0.5 as galaxies. At the redshifts of these groups, the typical seeing (0.8–1.5'') corresponds to  $\sim 3$ –10 kpc. Thus, we are unable to cleanly distinguish galaxies smaller than this size from stars. This has some impact on the selection of objects for our spectroscopic survey, although the effect appears to fairly small (based on the spectroscopy less than 10% of the targeted objects are stars). Priority was given to the brightest objects in each field. No color information was used to select spectroscopic candidates. This selection method has the advantage that it avoids biasing our study towards certain types of group galaxies (i.e. red galaxies), but comes at the price of a higher fraction of the spectroscopic targets being non-group members. Typically, three multi-slit masks were created for each group, with each mask containing between 15 and 20 objects.

All of the Palomar spectra were taken with the COSMIC spectrograph (Kells et al. 1999) on the 5.1m Hale telescope between 1999 and 2001. The instrument configuration resulted in spectra covering the wavelength range  $\sim 3500$ –9800 Å with a spectral scale of  $\sim 3.1$  Å/pixel. The two southern targets were observed with the WFCCD spectrograph on the du Pont 100-inch telescope at Las Campanas Observatory, Chile in October, 2000. The spectra cover the wavelength range  $\sim 3800$ –9500 Å with a spectral scale of  $\sim 4$  Å/pixel. A similar observing scheme was used for the COSMIC and WFCCD observations. Typically, two one-hour integrations were taken for each mask, with an arc and flatfield exposure taken at the completion of each mask exposure. A CuAr arc lamp was used for the COSMIC data and a HeNeAr lamp was used with the WFCCD. Finally, one group (RXJ0329.0+0256) was observed with LRIS (Oke et al. 1995) on Keck I during December 2004. The LRIS spectra are centered at  $\sim 6000$  Å and have a total wavelength range of  $\sim 2500$  Å.

The COSMIC and WFCCD data were reduced using IRAF. First, the overscan regions of the CCD chips were used to estimate and subtract the bias from each frame. Flatfield exposures were then used to construct a normalized flatfield frame by performing a low-order fit in the dispersion direction. The science frames were then divided by this normalized flatfield to correct for the pixel-to-pixel response of the detector. A distortion correction was applied to each frame to align the spectra along the rows of the detector. The positions of the objects on the slit and corresponding sky regions were then defined interactively using the IRAF package Apextract. The spectra were then sky-subtracted and extracted to produce one-dimensional spectra. Wavelength calibrations were determined for each spectrum from the arc exposures.

The LRIS spectroscopic data were reduced with custom scripts written to process multislit observations. The scripts serve as front ends to standard IRAF tasks. The processing included overscan subtraction, flat-field correction, cosmic-ray rejection, and sky subtraction. There were three science exposures obtained through each slitmask, with small dithers in

the spatial direction made between exposures. The background-subtracted science exposures for each slitmask were co-added, and then one-dimensional spectra were extracted from the combined two-dimensional files. The wavelength solutions were determined from arclamp exposures that were obtained immediately after the first science exposure for each slitmask.

Redshifts were measured using an IRAF script called `redsplot` (T. Small, private communication). This task allows the user to interactively identify a potential line feature in the spectrum and then plot the locations of other line features from a spectral line list. Redshifts are then measured from the centroid of each line. We adopt the average measurement from all of the line features as the final redshift for each object. The standard deviation of all of the measurements is used to estimate the error. The redshifts for all of the group members in this paper were based on a minimum of three distinct line features. More typically, five or six features were used for the redshift determination. In total, we measure redshifts for 169 galaxies. This corresponds to a  $\sim 65\%$  success rate. A significant fraction of the objects with measured redshifts have emission lines in their spectra ( $\sim 46\%$ ). However, the emission-line fraction among confirmed group members is much lower ( $\sim 20\%$ ). This result is not surprising given the large population of early-type galaxies that we find in these groups (§4.3). Many of the group members (63%) with emission lines have spectra consistent with the presence of an AGN. A detailed discussion of the emission-line properties of the group galaxies is deferred to a future paper.

### 3.2. Imaging Data

During the course of the Palomar and Las Campanas observing runs described above, images of each group were taken when conditions were photometric. The images were taken with a Kron-Cousins R filter from the Harris set. Typically, we took a series of nine five-minute exposures for each field, resulting in a total integration time of 45 minutes. The images were reduced using standard techniques in IRAF. The bias level was determined from the overscan region of the CCD and subtracted from the images. Flat-fielding was accomplished using dome flats. The images were flux-calibrated using observations of standard star fields from Landolt (1992). SExtractor (Bertin & Arnouts 1996) was used to measure a magnitude for each galaxy. We adopt the “MAG\_AUTO” option for our total magnitudes.

In addition to providing magnitudes, the R-band data were also used to determine the morphologies of the group members. Given the distances of these objects and the quality of these images it is generally not possible to make detailed morphological classifications with the groundbased data. For this reason, we restrict our classifications to “early” and “late” type galaxies. Each group member was visually classified by J.S.M. into one of the

two types. Higher resolution *Hubble Space Telescope* images taken with the *WFPC2* are available for all nine fields. However, given the small field of view of *WFPC2*, only about half of the spectroscopically confirmed group members were observed by *HST*. Independent classifications were made for each group galaxy observed with *HST*. In general, the agreement between the groundbased classifications and the *HST*-based classifications are good. There is a disagreement in the type in  $\sim 13\%$  of the galaxies. In all of these cases, the *HST* data suggest that a late-type galaxy has been misidentified as an early-type object. This is not too surprising because the *HST* images have the ability to reveal faint spiral structure that is not apparent in the lower resolution ground-based images.

Table 1 lists the J2000 coordinates, R-band magnitude, redshift, redshift error and type of redshift measurement (abs=absorption, em=emission and abs + em = combination of absorption and emission lines) for each galaxy in our survey with a measured redshift.

## 4. Results and Discussion

### 4.1. Group Membership

In most cases, the identification of the group in redshift space is trivial as the spatial distribution of galaxies on the sky coincide with the X-ray emission. However, for a few of these fields, there are several different galaxy systems superposed along the line of sight. This leads to some ambiguity about the true redshift of the X-ray system in two of the nine systems studied here. The RXJ1205.9+4429 field contains two significant galaxy systems, one at  $z \sim 0.35$  and another  $z \sim 0.59$ . The *XMM-Newton* observation of this field shows that the X-ray emission is clearly centered on a luminous early-type galaxy that is part of the  $z=0.59$  system (Paper II). Thus, we adopt this value as the redshift of this group. We note that the preliminary RDCS redshift corresponded to the lower redshift system. Therefore, the X-ray luminosity is actually considerably higher than originally reported in the RDCS. The true X-ray luminosity of this system is high enough that it does not meet our original selection criterion, suggesting this is likely a much richer system than the other objects in our sample. Ulmer et al. (2005) have recently published a detailed study of the X-ray and optical properties of this system and conclude that it is a fossil group. However, our spectroscopy and imaging data indicate that the magnitude difference between the brightest and second brightest confirmed member is  $\sim 1.2$  mag. in the R-band. Thus, this system is not a fossil group by the standard definition usually adopted in the literature (Jones et al. 2003).

In the case of RXJ0341-4459 field, we measure redshifts for five galaxies in a system at  $z \sim 0.41$ . The five galaxies have a spatial distribution similar to the X-ray emission.

However, there are also three foreground galaxies distributed over the same area. As these three objects have very different redshifts, they are not part of a single galaxy system. Thus, we believe the X-ray emission is most likely associated with the system at  $z \sim 0.41$ , although higher resolution X-ray images are required to be sure. Examples like this demonstrate the difficulty sometimes encountered when trying to identify low galaxy density systems (i.e. groups) at high redshift even when X-ray emission is present.

We determine group membership for each system using the ROSTAT package (Beers, Flynn & Gebhardt 1990). We start by considering all galaxies within  $\pm 3000 \text{ km s}^{-1}$  of the group's mean velocity. This is a large enough range to include all potential group members. We then calculate the biweight estimators of location (mean velocity) and scale (velocity dispersion). Objects with velocities greater than three times  $\sigma_{\text{biwt}}$  are then removed from the sample and a new mean location and scale are calculated. This process is repeated until there are no more objects to be clipped. This procedure resulted in the removal of one galaxy from three of the groups and none from the remainder. Figure 4 shows the velocity distributions of each member relative to the final mean velocity of the group. The final mean velocity and velocity dispersion are given in Table 2. For all of the systems studied here, the classical velocity dispersion (i.e.  $\sigma_{\text{Gauss}}$ , the Gaussian estimator) is in good agreement with the biweight velocity dispersion estimate. For approximately half of our sample, the velocity dispersions are based on only  $\sim 5$  velocity measurements. These velocity dispersions are rather uncertain. Studies of low redshift X-ray groups suggest velocity dispersions based on a small number of galaxies can be significantly underestimated (Zabludoff & Mulchaey 1998).

#### 4.2. The $L_X$ - $\sigma$ Relationship

Figure 5 shows the  $L_X$ - $\sigma$  relationship for our nine groups along with the sample of nearby groups from Osmond & Ponman (2004) and the moderate redshift X-ray groups from Willis et al. (2005). As can be seen from the figure, several of the groups fall significantly off the relationships found for nearby groups and clusters. The two most deviant points in our sample correspond to the RXJ1334.0+3750 and RXJ1648.7+6019 groups. These are the two groups from our *XMM-Newton* survey where the X-ray emission is not centered on an early-type BGG (Paper II). In both cases, these groups have very low velocity dispersions for their given X-ray luminosities. There are several possible explanations for why these groups fall so far off the relationships found for low redshift groups and clusters. First, our velocity dispersions estimates for these groups may be artificially low because they are based on relatively small numbers (6 and 8 members, respectively). Zabludoff & Mulchaey (1998) find

that velocity dispersions estimated from the five brightest galaxies can be underestimated by as much as a factor of three. A similar factor would bring our two most deviant groups in agreement with the relationship found for nearby groups and clusters. This idea can be tested by obtaining more velocity measurements. Second, the X-ray luminosities of these groups may have been enhanced or contaminated in some way. For example, the observed X-ray emission may be dominated by galaxy emission that is unresolved with our *XMM-Newton* observations. While we believe this is very unlikely given the high X-ray luminosities of our groups and the extent and morphology of the X-ray gas, we cannot rule this possibility out without higher resolution X-ray images. Thirdly, the velocity dispersions may have been reduced in some way. Helsdon, Ponman & Mulchaey (2005) have studied several nearby groups that fall off the  $L_X$ - $\sigma$  relationship in a similar manner to our groups (although the X-ray luminosities of the nearby groups are nearly two orders of magnitude lower than the present examples). They suggest several physical mechanisms that could reduce the velocity dispersions including dynamical friction and tidal heating. They also suggest that orientation effects can lead to an artificially low observed velocity dispersion. Finally, the low velocity dispersions could be an indication that these groups are in the process of collapsing for the first time and therefore the measured velocity dispersions do not yet accurately reflect the depth of the group potential (see Section 4.5).

### 4.3. Morphological Composition

Studies of X-ray groups at low redshift have revealed a very strong tendency for these systems to be dominated by early-type galaxies (Ebeling, Voges & Böhringer 1994; Pildis, Bregman & Evrard 1995; Henry et al. 1995; Mulchaey et al. 1996; Zabludoff & Mulchaey 1998). Table 2 lists the early-type fraction for our groups (based on the *HST* morphological classifications, where possible). For all but one of our objects, the early-type fractions are in the range  $\sim 0.4$ – $0.8$ . For the four groups with just four to six members known, these fractions could be somewhat over-estimated as our analysis is restricted to the brightest group members, which tend to be ellipticals (Zabludoff & Mulchaey 1998). However, even for the groups with many more members identified, the early-type fractions are comparable to those of rich clusters sampled out to similar radii (Whitmore, Gilmore & Jones 1993). Thus, the trend for X-ray groups to contain a large number of early-type galaxies appears to be in place out to at least  $z \sim 0.5$ . The one exception in our sample is the RXJ0210.4-3929 group, which based on the *HST* imaging is dominated by spiral galaxies. The large number of spirals in this system make it very unusual among X-ray groups at both low and moderate redshifts.

A correlation between early-type fraction and velocity dispersion has been noted for nearby group samples (Hickson, Kindl & Huchra 1988; Zabludoff & Mulchaey 1998; Osmond & Ponman 2004), suggesting that galaxy morphology is related to the depth of the group potential. For groups with well-determined membership, the relationship is surprisingly robust (Zabludoff & Mulchaey 1998). In Figure 6, we plot these quantities for our sample along with the low redshift data from Zabludoff & Mulchaey (1998). Among our moderate redshift groups, there is considerable scatter and no indication of a trend between early-type fraction and velocity dispersion. We suspect much of this scatter is an indication that neither quantity is well-determined for most of our groups. However, we note that the two groups in our sample with membership data comparable to that of the Zabludoff & Mulchaey (1998) sample (i.e.  $\sim 20$  known members) do appear to follow the trend found at low redshift. In fact, these two groups suggest that the relationship found by Zabludoff & Mulchaey (1998) extends to the range of poor clusters. As noted by Zabludoff & Mulchaey (1998), the relationship cannot be the same as for rich clusters as it would predict an unphysical early-type fraction for clusters with velocity dispersions above  $\sim 800$  km s $^{-1}$ .

#### 4.4. The Brightest Group Galaxy

Previous work on low redshift X-ray groups indicates that the X-ray emission is usually centered on a luminous elliptical galaxy (Ebeling, Voges & Böhringer 1994; Mulchaey & Zabludoff 1998; Helsdon & Ponman 2000; Mulchaey et al. 2003; Osmond & Ponman 2004). In almost every case, this elliptical is the most luminous galaxy in the group. As the peak in the X-ray emission is likely coincident with the center of the group potential, this implies that the brightest group galaxy (BGG) lies at the center of the potential.

Unfortunately, it is difficult to define the peak of the X-ray emission for the present sample from the low signal-to-noise *ROSAT* images. However, six of the nine groups have now been observed by *XMM-Newton* and four of these are consistent with the X-ray peak being coincident with the brightest group elliptical (Paper II). In all four groups with a central BGG, the radial velocity of the BGG is consistent with the mean velocity of the group within the velocity errors. Thus, similar to the case found for nearby X-ray groups (Zabludoff & Mulchaey 1998), the BGG is likely at or near the center of the group potential in these systems.

However, for three of the four groups where we find a dominant BGG, the central object appears to be composed of multiple nuclei (see Figure 7). In the two most spectacular cases (RXJ0720.8+7109 and RXJ1256.0+2556), the central object has three components. Although multiple nuclei in CD galaxies in clusters are fairly common (Hoessel 1980; Schnei-

der, Gunn & Hoessel 1983; Lauer 1988), in the majority of cases there is a large magnitude difference between the various components. In contrast, for both of our three nuclei systems, the second nuclei have R-band magnitudes within  $\sim 0.5$  mag. of the brightest component. In the case of the RXJ0720.8+7109 group, the second nucleus is the second brightest galaxy in the group. Previous studies of multiple nuclei in clusters have found large velocity offsets between the various components in some cases, indicating these systems are not bound and are thus not in the process of merging (Merritt 1984; Tonry 1985; Smith et al. 1985). For the RXJ0720.8+7109 group, we obtained a spectrum of the two brightest components and find a radial velocity difference of  $\sim 200$  km s $^{-1}$ . Given the typical errors on our velocity measurements ( $\sim 100$  km s $^{-1}$ ), our data are consistent with a similar radial velocity for the two components. Thus, the two components may be bound. For the other triple system, RXJ1256.0+2556, we only obtained a velocity for the central component, so we cannot infer anything further about the nature of the multiple nuclei.

As noted above, in only four of the nine groups in our sample is the X-ray emission clearly centered on an early-type galaxy. In two of the other groups the most luminous galaxy is an elliptical, but the existing X-ray data are not sufficient to determine an X-ray center (RXJ0341.9-4459 and RXJ1347.9+0752). Thus, we cannot draw strong conclusions for these two groups as to whether the X-ray emission is peaked on the dominant elliptical galaxy or not. For both groups, the brightest elliptical is offset in velocity from the mean velocity of the group by several hundred kilometers per second. However, we have very few velocity measurements for both systems, so the mean velocity of the group is not well-determined and we cannot draw strong conclusions regarding a potential offset of the BGG from the group center.

However, the remaining three groups in our sample deviate strongly from the low redshift trend for there to be a dominant elliptical galaxy at the center of the group potential. The RXJ1334.0+3750 group contains a dominant elliptical, but the peak of the X-ray emission is offset significantly from this galaxy (Paper II). The velocity of this galaxy is consistent with the mean velocity of the group within the errors on each measurement. However, given the very low velocity dispersion of this system ( $\sigma=121^{+58}_{-45}$ ) and the small number of known members (6), we cannot draw strong conclusions with the existing velocity data.

The most luminous galaxy in the RXJ1648.7+6019 group is also an elliptical, although the group contains several galaxies of comparable luminosity. Furthermore, the *XMM-Newton* data suggest the X-ray emission is not centered on any particular galaxy, but is instead distributed in a chain morphology similar to the distribution of galaxies near the group center (Paper II). The brightest elliptical is also offset in velocity from the mean velocity of the group by more than 200 km s $^{-1}$ . This provides further evidence that this galaxy

is not at the center of the group potential.

A chain-like morphology is also found in the RXJ0210.4-3929 group. In this case, the brightest galaxies in the chain are spirals. Unfortunately, we do not have *XMM-Newton* data for this system, so we cannot be sure where the X-ray emission peaks. Regardless, the most luminous early-type galaxy near the group center is nearly a magnitude fainter than the brightest spirals and has a velocity offset by nearly  $400 \text{ km s}^{-1}$  from the mean velocity of the group. Thus, this group also lacks a dominant central early-type galaxy.

#### 4.5. Evidence for Group Downsizing

As discussed in the last section, at least three (and potentially five) of the nine groups in the present sample do not appear to have a central dominant early-type galaxy. Furthermore, in three of the four groups where the X-ray emission is centered on a BGG, the central galaxy is not a single object, but rather is composed of multiple components. These observations suggest that most of the groups in our sample are not dynamically evolved. Instead, we appear to be catching them in the process of virialization.

The global X-ray properties of these groups are consistent with the properties of more dynamically relaxed systems, however (Paper II). This suggests that the X-ray properties of groups are already in place early in the formation of these systems. Specifically, the intragroup medium properties appear to be largely set prior to the BGG experiencing its last major merger and settling at the center of the group potential. This scenario would also explain the lack of evolution observed in the X-ray luminosity function of groups out to  $z \sim 0.5$  (Rosati et al. 1995; Jones et al. 2002; Willis et al. 2005) despite the morphological peculiarities we find over the same redshift interval. If true, the temperature of the hot gas component may provide a better indication of the global group potential early on than the velocity dispersion of the galaxies. This might explain the very low velocity dispersions observed for the RXJ1334.0+3750 and RXJ1648.7+6019 groups: The X-ray temperatures of these systems reflect the massive group potentials, but the velocity dispersions of the galaxies do not yet accurately probe the group mass. Cosmological simulations of groups that include both the intragroup gas and galaxies may be able to test this idea.

The late assembly of the BGG in groups is consistent with the results of simulations in hierarchical cosmological models (Dubinski 1998). The groups in our sample appear to cover a range in dynamical state and can therefore provide some clues into the formation process of the BGG. The RXJ0210.4-3929 and RXJ1648.7+6019 groups do not yet contain a dominant early-type galaxy and thus they are likely at the earliest stages of group formation.

The morphological compositions of these groups are very different, with RXJ0210.4-3929 consisting mostly of spirals and RXJ1648.7+6019 mostly of early-type galaxies. This suggests that both early and late type galaxies can be the dominant contributor to the final merger product. The groups with a multiple component BGG are likely much further along in the virialization process. In fact, the BGG in these groups is probably undergoing its final major merger. Finally, only one of the groups in our sample is consistent with being a relaxed, virialized system (RXJ0329.0+0256). In this case, the BGG is at the center of the group potential as determined from both the X-ray emission and the velocity distribution of the group members and is unlikely to undergo any more major mergers.

The fact that many of our intermediate redshift groups do not have a dominant central elliptical is somewhat surprising given that such groups appear to be very rare among local X-ray group samples (Mulchaey et al. 2003; Osmond & Ponman 2004). One potential concern in comparing our intermediate redshift groups to local samples is that the best studied local samples were not selected in a similar manner. In fact, the largest ROSAT surveys of groups were performed with very heterogeneous samples of groups mostly drawn from optical catalogs (Mulchaey 2000; Mahdavi et al. 2000; Helsdon & Ponman 2000; Mulchaey et al. 2003; Osmond & Ponman 2004). To allow a better comparison to low redshift systems, we have selected a sample of nearby X-ray groups and poor clusters from two surveys based on the *ROSAT* All-Sky Survey: the NORAS (Böhringer et al. 2000) and REFLEX (Böhringer et al. 2004) group and cluster samples. From each survey, we have selected all of groups and clusters with X-ray luminosities between  $\sim 2 \times 10^{42} h_{70}^{-2}$  ergs s $^{-1}$  and  $\sim 2 \times 10^{43} h_{70}^{-2}$  ergs s $^{-1}$  in the *ROSAT* band (i.e. the corresponding selection criterion for our intermediate redshift sample) with  $z \leq 0.05$ . Eliminating duplicate entries from the two catalogs produces a sample of 74 X-ray luminous groups and clusters. Unfortunately, the vast majority of these systems have not been previously studied in detail in either the optical or X-ray bandpasses. However, a literature search reveals that 19 of the 74 systems have deeper X-ray images published. The existing data for this subset of groups suggests these X-ray selected systems follow the trends found among the more heterogeneously selected nearby group samples. In particular, in all 19 of the groups, the X-ray emission is centered on a luminous early-type galaxy. Furthermore, we find no multiple-nuclei examples among the 19 nearby BGGs. This suggest that the differences we find between our intermediate redshift systems and local samples are not the result of a selection effect. Rather, the intermediate redshift groups appear to be less dynamically evolved than present day luminous X-ray groups.

A closer examination of low redshift samples suggests that there are some local examples of X-ray groups without a central BGG (Mulchaey et al. 2003; Osmond & Ponman 2004; Rasmussen et al. 2006). However, the X-ray luminosities of these systems are one to three orders of magnitude lower than the X-ray luminosities of our moderate redshift groups.

Among the  $\sim 60$  low redshift X-ray groups that have been studied in detail with *ROSAT*, the most luminous example of a system without a early-type BGG is the NGC 5171 group ( $L_X \sim 3 \times 10^{42}$  erg/s; Osmond & Ponman (2004)). Thus, among the most X-ray luminous ( $L_X > 5 \times 10^{42}$  erg s $^{-1}$ ) groups in the nearby universe, there appear to be no known counterparts to the systems we find at intermediate redshifts. The failure to find nearby examples of such systems suggests that the most X-ray luminous groups have largely reached virialization by  $z \sim 0$ . This suggest that we are witnessing group downsizing: While the most luminous (and thus most massive) groups are still in the process of virializing at intermediate redshifts, this process is restricted to much less luminous (and thus less massive) systems at the present day.

## 5. Summary

We have performed multi-object spectroscopy in the fields of nine candidate X-ray groups selected from the *ROSAT* Deep Cluster Survey. The velocity dispersions derived from our data span the range expected for groups and poor clusters. We have used ground-based and HST images of these fields to quantify the morphological compositions of these systems. We find that like low redshift X-ray groups, these systems contain a substantial population of early-type galaxies. Therefore, the large early-type fractions in X-ray groups are in place by at least  $z \sim 0.5$ .

In four of our nine groups, the X-ray emission is centered on a dominant early-type galaxy. In these cases, the velocity of the dominant galaxy is consistent with the mean velocity of the group, suggesting these galaxies are at the center of the group potential. However, in three of these four groups, the central galaxy is composed of multiple components, suggesting the BGG is still undergoing major mergers. This idea can be tested with more detailed spectroscopy of the multiple nuclei.

In at least three and potentially five of our groups, we find no evidence for a dominant central early-type galaxy. In several cases, a dominant elliptical exists, but it is not at the center of the group potential as determined by the X-ray emission or velocity distribution. In addition, two of the groups in the present sample do not contain a dominant early-type galaxy at all.

The fact that a large fraction of our intermediate redshift groups contain a BGG with multiple components or contain no central BGG at all suggests that these systems are not dynamically evolved. However, the X-ray properties of these systems are similar to those of nearby virialized groups, suggesting that the X-ray emission in groups likely reflects the

global properties of the potential earlier than the velocity distribution of the member galaxies. A comparison of our moderate redshift sample with similarly selected groups at low redshift indicates that the most X-ray luminous groups have reached a virialized state by the present time. However, there are examples of lower X-ray luminosity systems at low redshift that do not contain a central BGG. This may be evidence for group downsizing: While massive groups were still in the process of collapsing and virializing at intermediate redshifts, only lower mass systems are forming at the present time.

While the current study has uncovered some interesting results, much better data will be required to confirm our conclusions. We are in the process of obtaining higher quality spectroscopy for these systems which will allow a much more detailed analysis of their dynamical state and a first look at the properties of the individual galaxies in these groups.

We thank Roy Gal for advice on reducing the COSMIC data. We also acknowledge useful discussions with Alan Dressler, Mike Gladders, Daisuke Kawata and Dan Kelson. We also thank Somak Raychaudhury for suggestions that significantly improved this paper and Trevor Ponman for providing us with the fits to the GEMS data prior to publication. JSM acknowledges support from NASA grants NNG04GC846 and NNG04GG536 and HST grant G0-08131.01-97A.

*Facilities:* ROSAT, Du Pont, Hale, Keck, HST

## REFERENCES

Aarseth, S. J., & Fall, S. M. 1980, *ApJ*, 236, 43

Adami, C., Ulmer, M. P., Romer, A. K., Nichol, R. C., Holden, B. P., & Pildis, R. A. 2000, *ApJS*, 131, 391

Allington-Smith, J. R., Ellis, R., Zirabel, E. L., & Oemler, A. 1993, *ApJ*, 404, 521

Barnes, J. 1985, *MNRAS*, 215, 517

Beers, T., Flynn, K., & Gebhardt, K. 1990, *AJ*, 100, 32

Bertin, E., & Arnouts, S. 1996, *A&A*, 117, 393

Böhringer, H. et al. 2000, *ApJS*, 129, 435

Böhringer, H. et al. 2004, *A&A*, 425, 367

Burke, D. J., Collins, C. A., Sharples, R. M., Romer, A. K., Holden, B. P., & Nichol, R. C. 1997, *ApJ*, 488, 83

Burke, D. J., Collins, C. A., Sharples, R. M., Romer, A. K., & Nichol, R. C. 2003, *MNRAS*, 341, 1093

Carlberg, R. G. et al. 2001, *ApJ*, 552, 427

Cohen, J. G., Hogg, D. W., Blandford, R., Cowie, L. L., Hu, E., Songaila, A., Shopbell, P., & Richberg, K. 2000, *ApJ*, 538, 29

Dubinski, J. 1998, *ApJ*, 502, 141

Ebeling, H., Voges, W., & Böhringer, H. 1994, *ApJ*, 436, 44

Eke, V. R., Baugh, C. M., Cole, S., Frenk, C. S., King, H. M., Peacock, J. A. 2006, *MNRAS*, 362, 1233

Fassnacht, C. D., & Lubin, L. M. 2002, *AJ*, 123, 627

Faure, C., Alloin, D., Kneib, J. P., & Courbin, F. 2004, *AA*, 428, 741

Geller, M. J., & Huchra, J. P. 1983, *ApJS*, 52, 61

Gerke et al. 2005, *ApJ*, 625, 6

Grant, C. E., Bautz, M. W., Chartas, G., & Garmire, G. P. 2004, *ApJ*, 610, 686

Helsdon, S. F., & Ponman, T. J. 2000, *MNRAS*, 315, 356

Helsdon, S. F., Ponman, T. J., & Mulchaey, J. S. 2005, *ApJ*, 618, 679

Henry, J. P., et al. 1995, *ApJ*, 449, 422

Hickson, P., Kindl, E., & Huchra, J. P. 1988, *ApJ*, 331, 64

Hoessel, J. G. 1980, *ApJ*, 241, 493

Jeltema, T. et al. 2006, *ApJ*, in press (Paper II)

Jones, L. R., Scharf, C., Ebeling, H., Perlman, E., Wegner, G., Malkan, M., & Horner, D. 1998, *ApJ*, 495, 100

Jones, L. R., McHardy, I., Newsam, A., & Mason, K. 2002, *MNRAS*, 334, 219

Jones, L. R., Ponman, T. J., Horton, A., Babul, A., Ebeling, H., & Burke, D. J. 2003, MNRAS, 343, 627

Kells, W., Dressler, A., Sivaramakrishnan, A., Carr, D., Koch, E., Epps, H., Hilyard, D., & Pardeilan, G. 1999, PASP, 110, 1487

Landolt, A. U. 1992, AJ, 104, 340

Lauer, T. R. 1988, ApJ, 325, 49

Lubin, L. M., Postman, M., & Oke, J. B. 1998, AJ, 116, 643

Mahdavi, A., Böhringer, H., Geller, M. J., & Ramella, M. 2000, ApJ, 534, 114

Merritt, D. 1985, ApJ, 280, L5

Merritt, D. 1985, ApJ, 289, 18

Miles, T. A., Raychaudhury, S., Forbes, D. A., Goudfrooij, P., Ponman, T. J., & Kozhurina-Platais, V. 2004, MNRAS, 355, 785

Mulchaey, J. S. 2000, ARA&A, 38, 289

Mulchaey, J. S., Davis, D. S., Mushotzky, R. F., & Burstein, D. 1996, ApJ, 456, 80

Mulchaey, J. S., Davis, D. S., Mushotzky, R. F., & Burstein, D. 2003, ApJS, 145, 39

Mulchaey, J. S., & Zabludoff, A. I. 1998, ApJ, 496, 73

Nair, S. 2002, Journ. of Astron. & Astroph., 23, 115

Oke, J. B., et al. 1995, PASP, 107, 375

Osmond, J. P. F., & Ponman, T. J. 2004, MNRAS, 350, 1511

Perlman, E. S., Horner, D. J., Jones, L. R., Scharf, C. A., Ebeling, H., Wegner, G., & Malkan, M. 2002, ApJS, 140, 265

Pildis, R., Bregman, J., & Evrard, A. 1995, ApJ, 443, 514

Rasmussen, J., Ponman, T. J., Mulchaey, J. S., Miles, T. A., & Raychaudhury, S. 2006, MNRAS, submitted

Raychaudhury, S., Saha, P., & Williams, L. L. R. 2003, AJ, 126, 29

Romer, A. K., et al. 2000, ApJS, 126, 209

Rosati, P., Della Ceca, R., Burg, R., Norman, C., & Giacconi, R. 1995, *ApJ*, 445, L11

Rosati, P., Della Ceca, R., Norman, C., & Giacconi, R. 1998, *ApJ*, 492, L21

Rusin, D. et al. 2001, *ApJ*, 557, 594

Scharf, C. A., Jones, L. R., Ebeling, H., Perlman, E., Malkan, M., & Wegner, G. 1997, *ApJ*, 477, 79

Schneider, D. P., Gunn, J. E., & Hoessel, J. G. 1983, *ApJ*, 268, 476

Smith, R. M., Efstathiou, G., Ellis, R. S., Frenk, C. S., & Valentijn, E. A. 1985, *MNRAS*, 216, 71

Taylor, J. E., & Babul, A. 2005, *MNRAS*, 364, 515

Temporin, S., & Fritze-von Alvensleben, U. 2006, *A&A*, 447, 843

Tonry, J. L. 1985, *ApJ*, 291, 45

Turner, E. L., & Gott, J. R. III 1976, *ApJS*, 32, 409

Ulmer, M. P. et al. 2005, *ApJ*, 624, 124

Vikhlinin, A., McNamara, B. R., Forman, W., Jones, C., Quintana, H., & Hornstrup, A. 1998, *ApJ*, 502, 558

Whitmore, B., Gilmore, D., & Jones, C. 1993, *ApJ*, 407, 489

Williams, K. A. et al. 2006, *ApJ*, submitted

Willis, J. P. et al. 2005, *MNRAS*, 363, 675

Wilman, D. J., et al.(2005a), *MNRAS*, 358, 71

Wilman, D. J., et al.(2005b), *MNRAS*, 358, 88

Zabludoff, A. I., & Mulchaey, J. S. 1998, *ApJ*, 496, 39

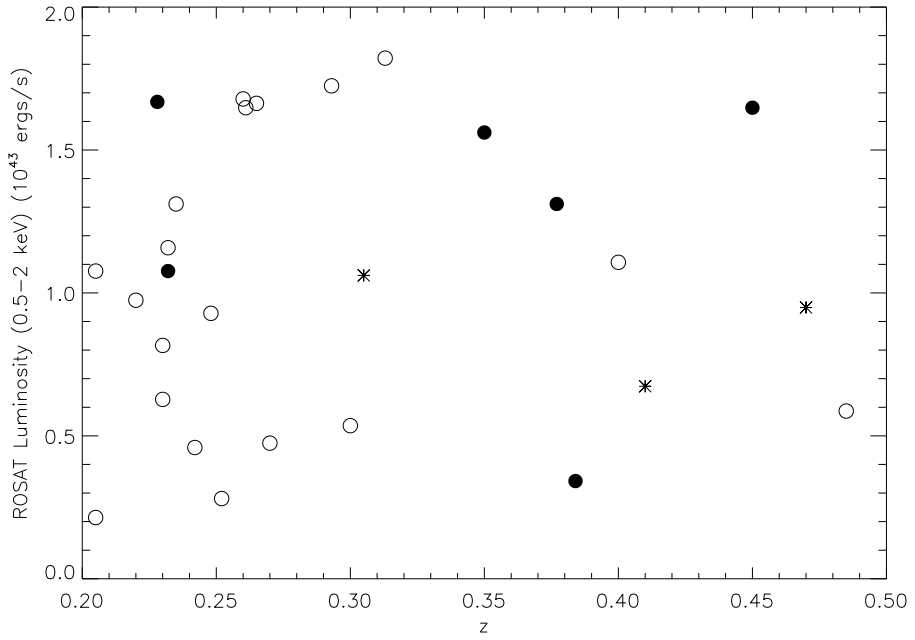


Figure 1 - Relationship between redshift and X-ray luminosity ( $L_X$ ) for the groups in the RDCS sample. Objects in the subsample discussed in this paper with *XMM-Newton* observations are shown as filled circles, while the groups in the present paper with only *ROSAT* observations are shown as stars. The redshifts and X-ray luminosities plotted are taken from the original RDCS survey.

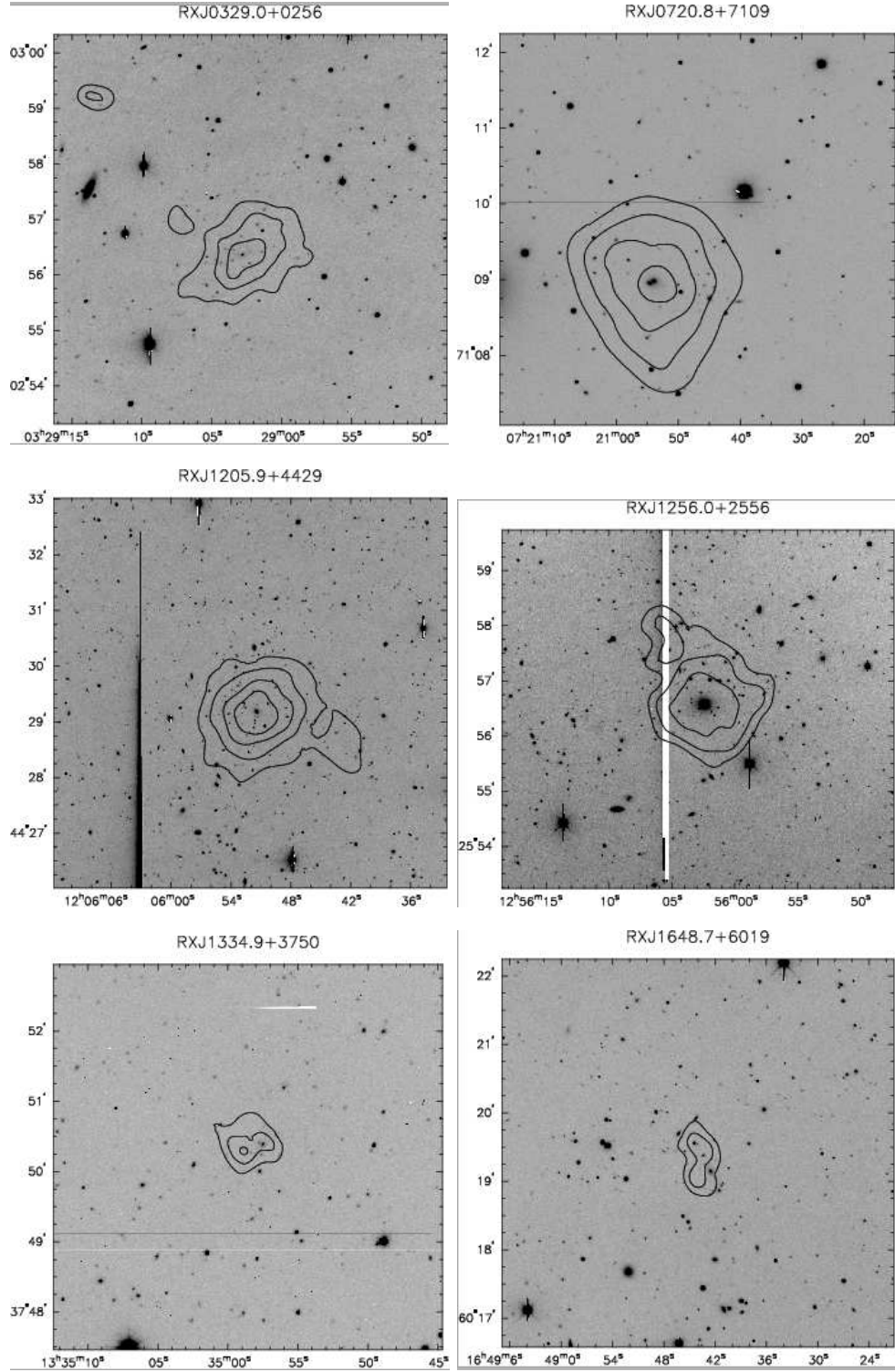


Figure 2 - *XMM-Newton* contours of the diffuse X-ray emission overlaid on optical images of the fields for the six systems with *XMM-Newton* data (Paper II). The contours correspond

to  $5\sigma$ ,  $10\sigma$ ,  $20\sigma$  and  $40\sigma$  above the background level.

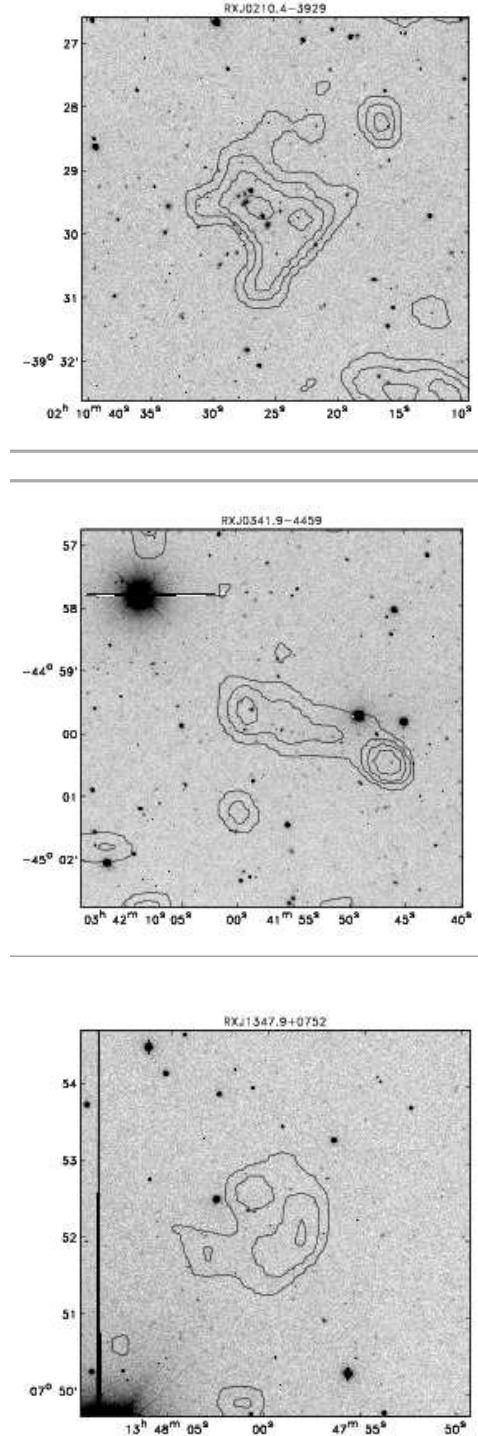
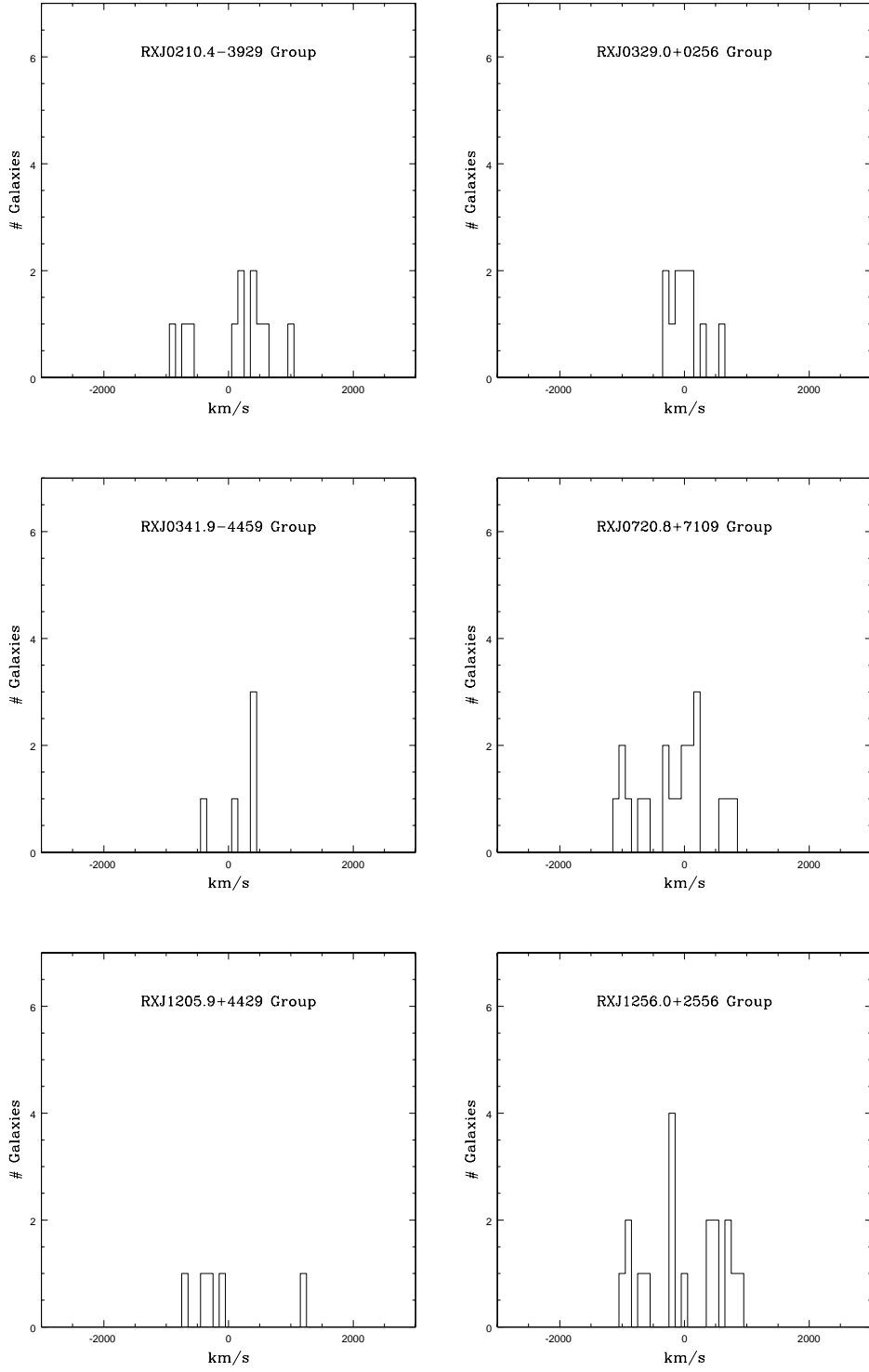


Figure 3 - *ROSAT* contours taken from the RDCS overlaid on optical images of the fields for the three systems in our sample without *XMM-Newton* data. The contours correspond

to  $3\sigma, 5\sigma, 7\sigma, 10\sigma$  and  $20\sigma$  above the background level.



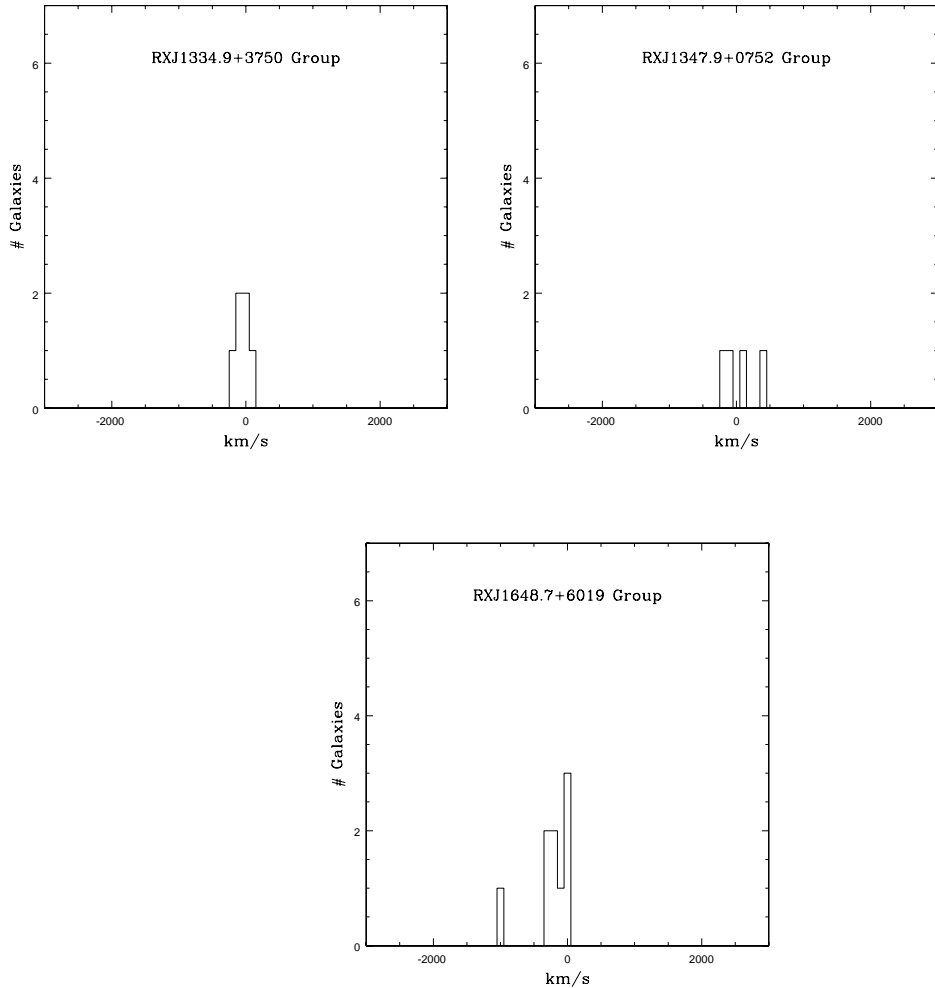


Figure 4 - Distribution of member velocities relative to the mean group velocity.

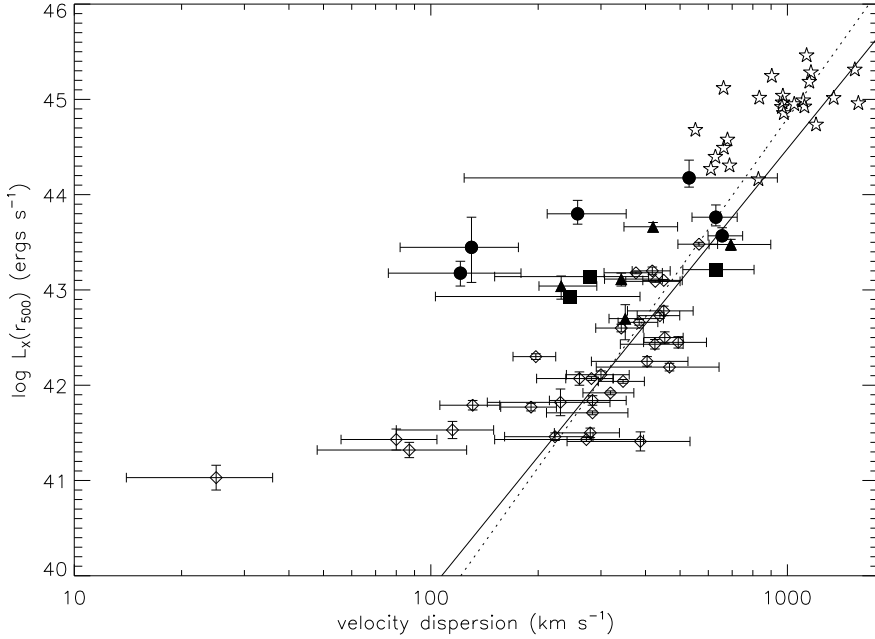


Figure 5 - Relationship between optical velocity dispersion and X-ray luminosity ( $L_x$ ) for the groups in the present sample with *XMM-Newton* observations (filled circles), the groups in our sample with only *ROSAT* observations (filled squares), the moderate redshift groups from Willis et al. (2005) (filled triangles) and the low redshift groups from Osmond & Ponman (2004) (open diamonds). For the *ROSAT*-only groups, a temperature of 2 keV has been assumed to estimate the X-ray luminosity. Also shown are a fit to the low redshift GEMS groups (solid line) and a fit to the Markevitch (1998) cluster sample (dotted line)(Helsdon & Ponman, in preparation).

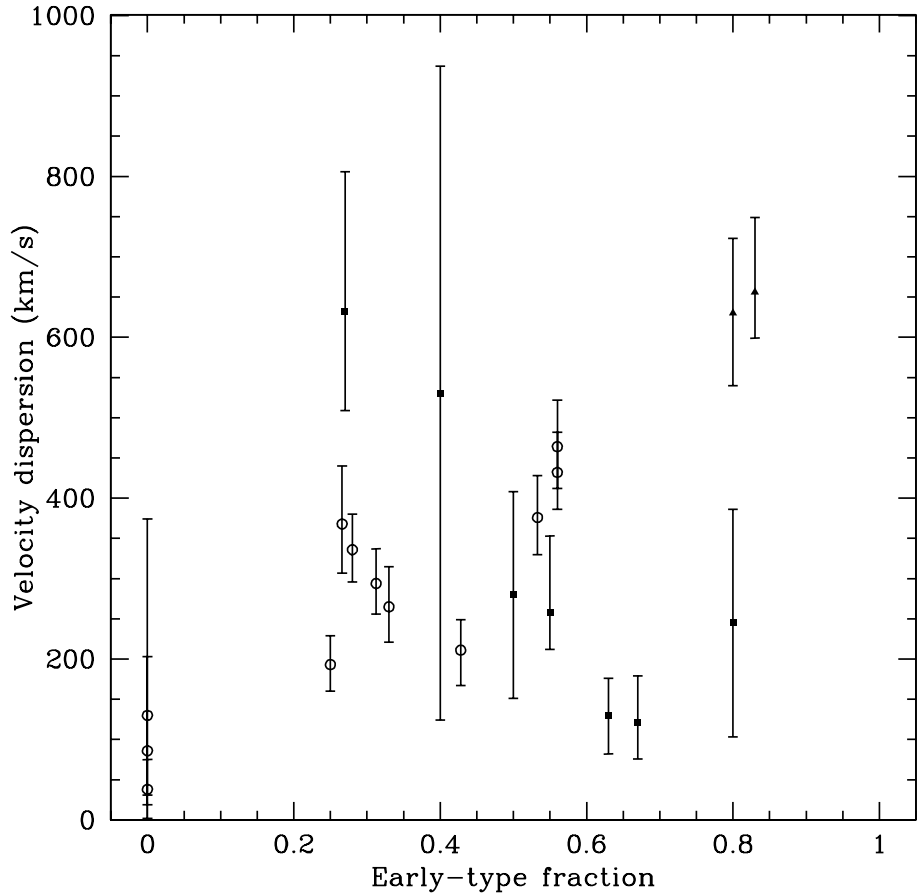


Figure 6 - Relationship between early-type fraction and optical velocity dispersion for the present sample (filled points) and the low redshift groups from Zabludoff & Mulchaey (1998) (open circles). The two groups from the current sample with the best membership data are plotted as triangles. Note that these two systems appear to extend the correlation found by Zabludoff & Mulchaey (1998) out to systems with velocity dispersions  $\sim 600$  km  $s^{-1}$ .

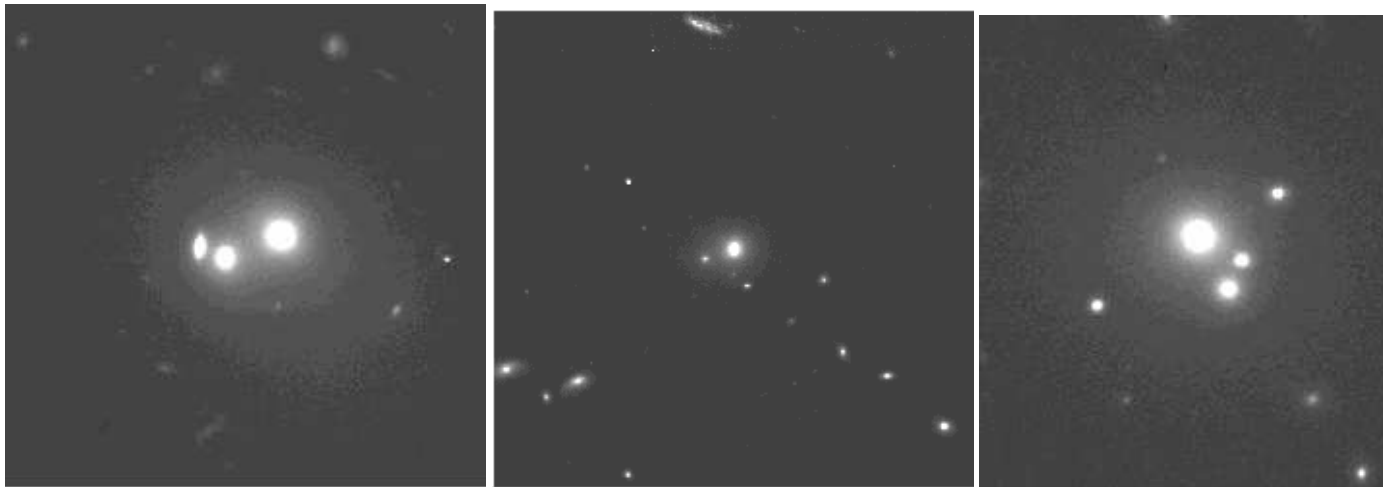


Figure 7 - *HST WFPC2* images of the centers of the RXJ0720.8+7109 (left), RXJ1205.9+4429 (middle) and RXJ1256.0+2556 (right) groups. The region plotted corresponds to a 200 kpc  $\times$  200 kpc region in each case.

Table 1. Photometric and Spectroscopic Results

RA (J2000)	Dec (J2000)	R mag.	z	z error	z type
02 10 09.90	-39 26 38.7	17.1	0.1659	0.0006	abs + em
02 10 10.78	-39 20 19.3	19.1	0.1758	0.0004	abs + em
02 10 13.39	-39 32 58.9	17.1	0.1665	0.0008	abs + em
02 10 14.40	-39 26 51.9	19.9	0.3025	0.0003	abs
02 10 14.98	-39 32 42.6	17.8	0.1678	0.0011	abs
02 10 21.10	-39 32 42.5	18.8	0.1643	0.0010	abs + em
02 10 21.71	-39 20 11.3	19.2	0.3702	0.0006	abs
02 10 24.52	-39 29 39.4	19.2	0.3075	0.0008	abs

Note. — The full table is available electronically.

Table 2. Group Properties

Group	RA (J2000)	Dec (J2000)	redshift	Members	$\sigma_{\text{biwt}}$	Early-type Fraction	Comments
RXJ0210.4-3929	02 10 24.89	-39 29 37.1	0.3058	11	$632^{+174}_{-123}$	0.27	No early-type BGG; spiral dominated
RXJ0329.0+0256	03 29 02.82	+02 56 25.2	0.4122	11	$258^{+95}_{-46}$	0.55	BGG at group center
RXJ0341.9-4459	03 41 56.83	-44 59 46.7	0.4063	5	$245^{+141}_{-142}$	0.80	BGG possibly offset in velocity
RXJ0720.8+7109	07 20 54.04	+71 08 57.9	0.2309	20	$630^{+93}_{-90}$	0.80	BGG with three components
RXJ1205.9+4429	12 05 51.44	+44 29 11.0	0.5926	5	$530^{+407}_{-406}$	0.40	BGG with two components
RXJ1256.0+2556	12 56 02.34	+25 56 37.1	0.2316	18	$656^{+93}_{-57}$	0.83	BGG with three components
RXJ1334.9+3750	13 34 58.95	+37 50 15.7	0.3839	6	$121^{+58}_{-45}$	0.67	BGG offset in X-rays and velocity
RXJ1347.9+0752	13 47 59.51	+07 52 12.1	0.4649	4	$280^{+128}_{-129}$	0.50	BGG possibly offset in velocity
RXJ1648.7+6019	16 48 43.63	+60 19 21.5	0.3763	8	$130^{+46}_{-48}$	0.63	No dominant BGG; brightest early-type